IJBMS

Characterization of exosomes from hypoxia-activated human amniotic membrane mesenchymal stem cells

Hadiseh Kholgh [1#], Fatemeh Eshghabadi [2#], Hanieh Jafary [1], Kavosh Zandsalimi [3], Nazanin Akbari [4], Azadeh Soltani [5], Banafsheh Heidari [6*]

[1] Department of Biology, Science and Research Branch, Islamic Azad University, Tehran, Iran
[2] Department of Life Science Engineering, College of Interdisciplinary Science and Technology, University of Tehran, Tehran, Iran
[3] Department of Medical Laser (MLRC), Medical Laser Research Center, Yara Institute, ACECR, Tehran, Iran
[4] Department of Biology, Shahid Beheshti University, Tehran, Iran
[5] Reproductive Biotechnology Research Center, Avicenna Research Institute, ACECR, Tehran, Iran
[6] Department of Regenerative Medicine in Wound Healing, Medical Laser Research Center, Yara Institute, ACECR, Tehran, Iran

ABSTRACT

Objective(s): Hypoxia is a physical stimulus that enhances stem cell activities to produce more cellular derivatives, particularly exosomes. Enhancing the quantity and quality of exosomes can improve their therapeutic properties. The study aimed to evaluate the effects of normoxic ($22\%O_2$) and hypoxic ($1\%O_2$) conditions on the characteristics of amniotic membrane-derived mesenchymal stem cells (AM-MSCs) and their exosomes.

Materials and Methods: AM-MSCs were isolated, confirmed, and cultured under normoxic and hypoxic conditions. Exosomes were extracted from AM-MSCs and assessed for morphological characteristics (size/distribution/surface topography), structural properties (aggregation/colloidal particle behavior/surface charge/stability), chemical features (functional groups/ionic interactions), biological capacities (total protein concentration) and biocompatibility (microbiological quality/cytotoxicity/irritation/sensitization).

Results: Hypoxia did not adversely affect the stemness potential of AM-MSCs ($P>0.05$). The average sizes of exosomes derived from AM-MSCs (AM-MSCs-Exo) were 185.7±23 nm (PI=0.756) and 145.4±36 nm (PI=0.420) under normoxic and hypoxic conditions, respectively ($P\leq0.05$). Zeta potential of AM-MSCs-Exo was -2.57±0.5 mV under normoxia, while it was -2.37±0.73 mV in the hypoxic conditions. Exosomes from hypoxia-treated cells exhibited greater uniformity, dispersion, and stability than those from the normoxic group, resulting in reduced fluctuation under scattered light over time ($P\leq0.05$). The total protein concentration in the hypoxic group was significantly higher than in the normoxic conditions (5.003 mg/ml vs. 4.109 mg/ml, representing a 1.22-fold increase) ($P\leq0.01$). Exosomes extracted under normoxic and hypoxic conditions demonstrated acceptable biocompatibility with no signs of cytotoxicity, irritation, sensitivity, or microbial contamination.

Conclusion: Hypoxic preconditioning enhances the yield and physicochemical stability of AM-MSC-derived exosomes, due to their unique composition and functional properties.

▶ Please cite this article as:
Kholgh H, Eshghabadi F, Jafary H, Zandsalimi K, Akbari N, Soltani A, Heidari B. Characterization of exosomes from hypoxia-activated human amniotic membrane mesenchymal stem cells. Iran J Basic Med Sci 2026; 29:

Introduction

Mesenchymal stem cells (MSCs) are widely recognized as the most common multipotent stem cells in tissue engineering and regenerative medicine. Their ability to differentiate into various cell lines, immunomodulatory effects, high proliferation potential, and secretion of various paracrine factors result in their wide applications in cell therapy and cell-free therapies (1-3). MSCs can be isolated from various tissues, such as skin (4), adipose tissue (5), bone marrow (6), dental pulp (7), amniotic membrane (8), liver (9), urine (10), etc. MSCs from different sources have distinct cellular characterization and secretory properties, including paracrine bioactive factors (3, 9). Variation in bioactive factors across different sources makes it possible to use them in a wide range of therapeutic applications, particularly cell-free therapies. Since 2014, cell-free therapy (especially cell derivatives) has been widely used in various therapeutic fields (11). Cell derivatives (especially exosomes and/or ectosomes) have several advantages, including non-toxicity, less immune response in recipients, cost-effectiveness, simplified storage without any cryoprotectant components, easier transportation, etc. Treating with exosomes and/or ectosomes decreases the risk of infectious transmission, engraftment failure, embolization, and tumorigenesis, making it suitable for allogeneic transplantation. Furthermore, in emergency cases like brain ischemia and myocardial infarction, where time is critical, cell-free therapy is more effective than cell therapy (12-17).

Cell derivatives contain two distinct fractions: vesicular and soluble fractions. The vesicular fraction comprises various types of extracellular vesicles (EVs), with ectosomes making up a significant portion of these EVs. Ectosomes originated from the direct budding of the plasma membrane, unlike exosomes, which are generated through the endosomal pathway (do not originate from intracellular membrane-bound structures or organelles). Ectosomes encompass a broad population of EVs that originated from the direct budding of the plasma membrane, unlike exosomes, which are generated through the endosomal pathway (do not originate from intracellular membrane-bound structures or organelles). These vesicles exhibit a wide range of sizes from 50 nm to 1 mm, occasionally overlapping with the exosomes' dimensions (18). One of the most important functional or biologically active components in cell derivations is the exosome, an extracellular vesicle with a diameter of 40–160 nm. This microvesicle contains various receptors, enzymes, lipids, proteins, DNA, miRNAs, mRNAs, etc. Exosomes can be classified into several categories based on their size, content, and functional effects. According to their size, exosomes can be categorized into three distinct classes: Exo A, which ranges from 40 to 75 nm; Exo B, measuring between 75 and 100 nm; and Exo C, with a size from 100 to 160 nm. Based on their effects on the recipient cells, exosomes are grouped into Exo α (providing pro-survival signals), Exo β (providing pro-apoptotic signals), and Exo γ (providing immunomodulation signals) (19). There are several approaches for isolating exosomes from stem cells, including differential ultracentrifugation, sucrose density gradient centrifugation, iodixanol density gradient centrifugation, filtration, and size exclusion chromatography (20-23). To enrich exosomes in cell derivations and enhance their therapeutic applications, several methods have been developed, including serum starvation (24), glucose starvation (25), and hypoxia (26). Hypoxia is a condition characterized by a decreased oxygen concentration in the environment, resulting in alterations and modifications in cellular behaviors and the secretion of paracrine factors. This condition increased exosome release, enhanced the expression of bioactive molecules such as hypoxia-inducible factors (HIFs) and other biomarkers, and improved miRNA biological functionality, which promotes angiogenesis and cellular uptake efficiency (26-32). So far, hypoxia-induced exosomes have been studied in some therapeutic fields, including bone fracture (33), chronic wound healing (34), nervous regeneration (29), anti-tumor immunity, immunotherapy (35), and cancer diagnosis (36).

This study aimed to evaluate the effect of the hypoxic condition (1% O_2) on the morphological characteristics (shape, size, distribution, surface topography, and agglomeration), structural properties (aggregation, homogeneity, colloidal particle behavior, surface charge, and stability), chemical feature (functional groups and ionic interactions), biological capacities (total protein concentration, and cytotoxicity), and biocompatibility (microbiological quality, systemic toxicity, irritation and sensitization) of exosomes extracted from the amniotic membrane-mesenchymal stem cells (AM-MSCs) using Fourier-Transform Infrared Spectroscopy (FTIR), Scanning Electron Microscopy (SEM), Transmission Electron Microscopy (TEM), Dynamic Light Scattering (DLS), Zeta potential, and BCA.

Materials and Methods
All materials, unless otherwise noted, were obtained from Sigma Aldrich (St. Louis, MO, USA). All experiments were approved by the Ethics Committees at the Research Ethics Committees of Islamic Azad University, Science and Research Branch (approval ID: IR.IAU.SRB.REC.1403.081). Human placentas were collected from healthy donors according to specific inclusion and exclusion criteria through selective cesarean at the Gandhi-Hotel Hospital, Tehran, Iran. Inclusion criteria include age between 30 and 60 years, full-term pregnancy (38-40 weeks), no drug addiction, metabolic diseases, liver disorders, bacterial and mycoplasma infections, and viral infections such as HIV-1/2 Ab, HBV, HCV, syphilis, and HPLV. All tissue samples were collected with the patient's informed consent and transferred to the laboratory at 4 °C.

Isolation and identification of AM-MSCs
Preparation of the amniotic membrane, isolation, and characterization of MSCs were performed based on the study by Heidari et al. in 2025, with minor modifications (37). Briefly, five human placentas were collected in sterile bags and transported to the laboratory on ice (4 °C) for 20 min. The fetal part of the placenta was rinsed with phosphate-buffered saline (PBS) supplemented with 100 IU/ml penicillin and 100 mg/ml streptomycin. Then, the amniotic membrane was carefully separated from the chorion by mechanical manipulation and extensively rinsed with PBS containing antibiotics (100 μg/ml penicillin, 100 μg/ml streptomycin) to remove any residual blood and mucus. The amniotic membrane was cut into 1cm, digested with collagenase IA for 35–40 min, and centrifuged at 1200 ×g for 10 min at 25 °C. The pellet was suspended in DMEM (Dulbecco's Modified Eagle Medium)/F12 supplemented with 10% FBS (Fetal Bovine Serum), 3 mM GlutaMAX, 1% Non-Essential Amino Acid Solution (NEAA), 100 IU/ml penicillin, and 100 mg/ml streptomycin and passed through a 70 μm nylon mesh. The harvested cells were cultured at a concentration of 10^6 cells/ml in 75 cm² culture flasks and incubated at 37 °C and 5% CO_2 for 5 days. The culture medium was changed every 3 days until the cells reached a density of 80–90%. Then, the confluent cells were trypsinized using 0.05% trypsin/EDTA and propagated until passage 3.

Study design
AM-MSCs at passage 3 were randomly divided into the control (normoxia) and experimental (hypoxia) groups. In the normoxic group, AM-MSCs at a concentration of $2×10^6$ cells were suspended in a T75 culture flask containing DMEM/F12 supplemented with 10% exosome-depleted FBS (Exo-free FBS, ThermoFisher, Waltham, MA, USA), 1% NEAA, 3 mM GlutaMAX, 100 IU/ml penicillin, and 100 mg/ml streptomycin at 37 °C and 5% CO_2, 22% O_2 for 72 hr. In the hypoxic group, AM-MSCs at the same concentration ($2×10^6$ cells/each T75 culture flask) were cultured in DMEM/F12 with 10% exosome-depleted FBS, 1% NEAA, 3 mM GlutaMAX, 100 IU/ml penicillin, and 100 mg/ml streptomycin for 48 hr at 37 °C, 22% O_2, and 5% CO_2. Subsequently, the culture flasks were placed in an incubator with 1% O_2, 5% CO_2, and 37 °C for an additional 24 hr (37-39). Cell propagation in each experimental condition (hypoxia and normoxia) was independently repeated 17-20 times to ensure reproducibility and to generate sufficient

conditioned media for subsequent exosomes extraction.

Stemness potential of AM-MSCs in different culture conditions

To investigate the effect of normoxia and hypoxia on the stemness potential of AM-MSCs, we evaluated the expression of MSC-specific molecular markers, as described in the protocol previously established by Heidari *et al.* (37). For this purpose, the expressions of CD105, CD73, CD90, CD29, CD34, CD45, and CD14 molecular markers were detected in different groups using a flow cytometer.

Preparation of AM-MSCs-Exosomes in the normoxic and hypoxic conditions

Exosomes were isolated from the conditioned media of AM-MSCs in both the normoxic and hypoxic groups using a differential ultracentrifugation method, following a protocol previously described by Karimi *et al.* (38). For this purpose, the conditioned media in different groups were separately collected and centrifuged at 300×g for 10 min at 4 °C. After discarding the pellet, the supernatant was centrifuged again at 2000×g for 10 min at 4 °C, followed by a second centrifugation at 10,000×g for 30 min at 4 °C. After serial centrifugations, the supernatant was filtered through a 0.22 μm nylon mesh and subsequently underwent two rounds of centrifugation at 100000×g for 70 min at 4 °C. Following centrifugation, the exosome pellet was carefully resuspended in cold PBS and immediately stored at -80 °C for future analyses. To ensure reproducibility and obtain sufficient concentration of exosomes for subsequent analyses, the ultracentrifuge-based extraction method was independently repeated at least 15 times for each group.

SEM and TEM

The morphological characteristics, including size, internal structure, and topography, of AM-MSCs-Exo in the control and experimental groups were analyzed using SEM and TEM, as described previously by Karimi *et al.* (38). For SEM analysis, AM-MSCs-Exo were fixed in 2% paraformaldehyde and diluted in distilled water. Then, suspension (5 μl) was placed on a silicon chip and immersed in acetone for dehydration. After rinsing and drying, SEM was conducted at a selective voltage of 30k using an MIRA3 Microscope (TESCAN, Czech). After rinsing and drying, SEM imaging was performed using a MIRA3 Microscope (TESCAN, Czech) at a voltage of 30 kV. At least three images at different angles were analyzed using magnifications of 500 nm, 5 μm, and 20 μm.

For TEM analysis, the exosome suspension was treated with 1% glutaraldehyde and placed as droplets on carbon-coated grids. After drying, they were rinsed twice in sterilized PBS for 1 minute. The samples were then stained with 1% uranyl acetate for 16 min. Three images from different angles were taken at a magnification of 50 nm using a Philips CM-120 Microscope (Netherlands) set to a voltage of 100kV.

FTIR

FTIR spectroscopy revealed the functional groups and molecular composition of exosomes through their infrared absorption profiles. Spectral investigation for AM-MSCs-Exo in the normoxic and hypoxic groups was collected in the range of 400-4000 cm^{-1} using an AVATAR spectrometer (Thermo, USA). This analysis determined the biochemical composition of AM-MSCs-Exosomes, highlighting the similarities and differences in the molecular structure between the experimental groups. All measurements were performed in triplicate to ensure reproducibility.

DLS and Zeta potential

The particle size, distribution, surface charge, and electrostatic potential of AM-MSCs-Exo in the normoxic and hypoxic groups were detected using DLS and Zeta potential measurements with the HORIBA SZ-100 system (Horiba Jobin Yvon, Japan). For this purpose, AM-MSCs-Exo were diluted in PBS (1:5) and sonicated on ice for 20 min for homogenization. Zeta potential measurements were conducted under the following conditions: pH 7.4, 25 °C, and 2.7 V. All measurements were performed in triplicate to ensure reproducibility and reliability of the data (38, 39).

BCA Assay

To determine the total protein concentration of AM-MSCs-Exo, the BCA assay was utilized. The principle of this assay is the reduction of copper (II) to copper (I), and BCA binds to copper (I). This reaction results in a purple color, which can be quantified by measuring the absorbance at 562 nm. For the assay, 1 mg of standard protein (Albumin) was dissolved in 1 ml of distilled water. To prepare the standard samples, different proportions of BSA and distilled water were mixed in a volume of 10 μl in a 96-well plate. Approximately 10 μl of the experimental samples (normoxic and hypoxic groups) were added to the well in three replicates. Then, the reagents (A and B) were combined in a 2:100 ratio. After mixing, 100 μl of the reagent mixture was added to each well, and the plate was incubated for 30 min at 37 °C. Following the incubation period, the optical density (OD) was measured three times at 562 nm, allowing the quantification of protein concentration in the exosomes derived from amniotic membrane-MSCs.

Biocompatibility

The biocompatibility of AM-MSCs-derived exosomes was investigated through a series of comprehensive assessments, including microbial contamination, potential toxicity, irritation, and sensitization. To ensure reproducibility and reliability of the tests, microbial contamination and toxicity were performed at least three times independently. Additionally, irritation and sensitization tests were conducted using three male New Zealand rabbits and six male Albino guinea pigs.

Microbiological examination

The bioburden test was conducted in accordance with the United States Pharmacopeia 2024 guidelines (40). For this purpose, the AM-MSCs-Exo extracts from both normoxic and hypoxic conditions were microbiologically evaluated by Nikopharmed's laboratories, a reputable partner of the Food and Drug Administration (FDA) with official accreditation from the National Accreditation Center of Iran (NACI). The AM-MSCs-derived exosomes in different groups were inoculated in nutrient broth or peptone broth carrier solution using a sterile swab and cultured on blood agar, EMB, and Chocolate Agar media to determine the presence or absence of Gram-positive or Gram-negative bacteria. Total aerobic microbial count (TAMC) was detected using Soybean-Casein Digest Agar (TSB) plates for 3 days at 30–35 °C. To determine the total combined yeasts and molds

count (TYMC), Sabouraud Dextrose Agar (SDB) plates were incubated at 20–25 °C for 5 days.

The product passes the tests if colonies of specified types are absent or if confirmatory identification tests are negative. The evaluation of the product's growth-promoting and inhibitory properties was conducted in accordance with the USP 2024 guidelines, utilizing a negative control to ensure valid testing conditions. Acceptance criteria were established based on either individual test results or the average counts from replicate tests. Table 1 outlines the acceptance criteria for the microbiological quality of exosomes, derived from the average of three replicate counts to enhance accuracy and reliability.

Cytotoxicity assay

To assess the cytotoxicity of exosomes in both normoxic and hypoxic conditions, an MTT assay was performed according to the guidelines outlined in ISO 10993-5 and ISO 10993-12. For this purpose, four various concentrations of exosomes (5, 10, 15, and 20 µg/ml) were prepared in cold PBS. L-929 fibroblast cells were seeded at a concentration of 1×10^4 cells/well in a 96-well culture plate using DMEM supplemented with 10% exosome-depleted FBS, and incubated for 24 hr at 37 °C, 5% CO_2, and 22% O_2. After initial incubation, the culture medium was carefully replaced with fresh medium containing various concentrations of exosomes derived from the normoxic and hypoxic groups. The cells were incubated for an additional 24 hr at 37 °C, 5% CO_2, and 22% O_2. Following incubation, the culture medium was removed, and 0.5 mg/ml MTT reagent (3-(4,5-dimethylthiazol-2-yl)-2,5-diphenyltetrazolium bromide) was added to each well for 4 hr. Afterward, isopropanol was added to dissolve formazan crystals. The optical densities of wells were detected at 570 nm.

In vivo irritation test

An *in vivo* irritation test for AM-MSCs-Exosomes under normoxic and hypoxic conditions was performed according

to ISO 10993-10 using three male New Zealand rabbits. Sample preparation followed the standard methods in ISO 10993-10 and ISO 10993-12. The backs of the animals were completely shaved, and four sites were marked as shown in Figure 1, including AM-MSCs-Exo hypoxia (site 1), AM-MSCs-Exo normoxia (site 2), control 1 (no injection, Site 3), and control 2 (normal saline injection, site 4). Approximately 0.5 ml of AM-MSCs-derived exosomes at a concentration of 20 µg/ml from normoxic and hypoxic groups were intradermally injected into sites 1 and 2, respectively. Site 3 received 0.5 ml of normal saline as a control, while site 4 remained untreated (no injection). All sites were covered with a non-occlusive dressing for 4 hr. The sites were evaluated for edema, erythema, and eschar formation at 4, 24, 48, and 72 hr. Tables 2 and 3 demonstrate the scoring system and the primary or cumulative irritation index for the rabbits.

In vivo sensitization assay

An in vivo irritation test for AM-MSCs-Exosomes under normoxic and hypoxic conditions was performed according to ISO 10993-10 using three male New Zealand rabbits. Sample preparation followed the standard methods in ISO 10993-10 and ISO 10993-12. Figure 2 illustrates the injection sites and corresponding solutions for each group. According to ISO 10993-10, a total of six male Albino guinea pigs
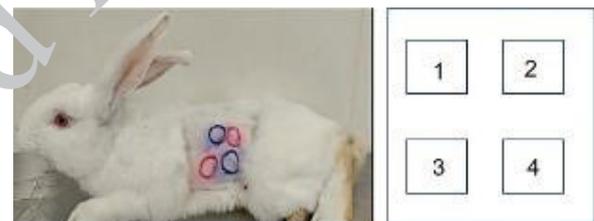
Figure 1. Intradermal injection sites on the rabbits' backs
AM-MSCs-Exo normoxia (site 1), AM-MSCs-Exo hypoxia (site 2), control 1 (Site 3), and control 2 (site 4).

Table 1. Acceptance criteria for microbiological quality of exosomes

1,,0	TAMC (CFU/g or CFU/ml)	TYMC (CFU/g or CFU/ml)	Specified micro-organism(s)
Non-aqueous preparations for oral use	10^3	10^2	Absence of *Escherichia coli* (1 g or 1 ml)
Aqueous preparations for oral use	10^2	10^1	Absence of *E. coli* (1 g or 1 ml)
Rectal use	10^3	10^2	-
Oromucosal use	10^2	10^1	Absence of *Staphylococcus aureus* (1 g or 1 ml) Absence of *Pseudomonas aeruginosa* (1 g or 1 ml)
Gingival use	10^2	10^1	Absence of *S. aureus* (1 g or 1 ml) Absence of *P. aeruginosa* (1 g or 1 ml)
Cutaneous use	10^2	10^1	Absence of *S. aureus* (1 g or 1 ml) Absence of *P.* aeruginosa (1 g or 1 ml)
Nasal use	10^2	10^1	Absence of *S. aureus* (1 g or 1 ml) Absence of *P, aeruginosa* (1 g or 1 ml)
Auricular use	10^2	10^1	Absence of *S. aureus* (1 g or 1 ml) Absence of *P. aeruginosa* (1 g or 1 ml)
Vaginal use	10^2	10^1	Absence of *P. aeruginosa* (1 g or 1 ml) Absence of *S. aureus* (1 g or 1 ml) Absence of *Candida albicans* (1 g or 1 ml)
Transdermal patches (limits for one patch, including adhesive layer and backing)	10^2	10^1	Absence of *S. aureus* (1 patch) Absence of *P. aeruginosa* (1 patch)
Inhalation use (special requirements apply to liquid preparations for nebulization)	10^2	10^1	Absence of *S. aureus* (1 g or 1 ml) Absence of *P. aeruginosa* (1 g or 1 ml) Absence of bile-tolerant gram-negative bacteria (1 g or 1 ml)

TAMC; Total aerobic microbial count; TYMC; Total combined yeasts and molds; CFU; Colony-forming unit

Table 2. Scoring system for erythema and edema in rabbits

	Reaction	Irritation score
Erythema and Eschar Formation	No erythema	0
	Very slight erythema (barely perceptible)	1
	Well-defined erythema	2
	Moderate erythema	3
	Severe erythema (beet-redness) to eschar formation, preventing grading of erythema	4
Edema Formation	No edema	0
	Very slight edema (barely perceptible)	1
	Well-defined edema (edges of the area well-defined by definite raising)	2
	Moderate edema (raised approximately 1 mm)	3
	Severe edema (raised more than 1 mm and extending beyond the exposure area)	4
	Maximal Possible Score for Irritation	8

Table 3. The primary or cumulative irritation indices in the rabbits

Mean score	Response category
Negligible	0 to 0.4
Slight	0.5 to 1.9
Moderate	2 to 4.9
Severe	5 to 8

were used for *in vivo* sensitization of exosomes and divided into two groups. Three guinea pigs received AM-MSCs-Exo under normoxic (A1, A2, A3) and hypoxic (B1, B2, B3) conditions, while the other three guinea pigs received normal saline (C1, C2, C3) and no injection (D1, D2, D3). For injection, the backs of the animals were completely shaved, and 0.1 ml of normal saline (C1-3) or exosomes containing 20 µg/ml (A1-3 and B1-3) were injected intradermally in the clipped intrascapular region (Figure 2). All sites were covered with a non-occlusive dressing for 4 hr. The sites were evaluated for edema, erythema and eschar formation at 4, 24, 48, and 72 hr. Tables 2 and 3 demonstrate the scoring system and the primary or cumulative irritation index for the rabbits.

Statistical analysis

Quantitative data are represented as means ± standard deviation (SD), while qualitative data are expressed as frequency and percentage. Statistical analysis was performed using GraphPad Prism 9 (GraphPad, USA) and SPSS 16 (IBM Corporation, USA). Group comparisons were performed using independent T-tests, paired t-tests, and Wilcoxon tests, as appropriate. One-way ANOVA was applied for multiple group comparisons. A *P*-value of ≤0.05 was considered statistically significant.

Results

Effect of hypoxic and normoxic conditions on the stemness potential of AM-MSCs

Figure 3 shows the expressions of CD105, CD73, CD90, CD34, CD45, CD29, and CD14 molecular markers in AM-MSCs propagated under normoxic (A-F) and hypoxic (a-f) conditions using flow cytometry. There are no significant differences in the expressions of positive biomarkers (CD105, CD73, CD90, and CD29) and CD45, and CD14
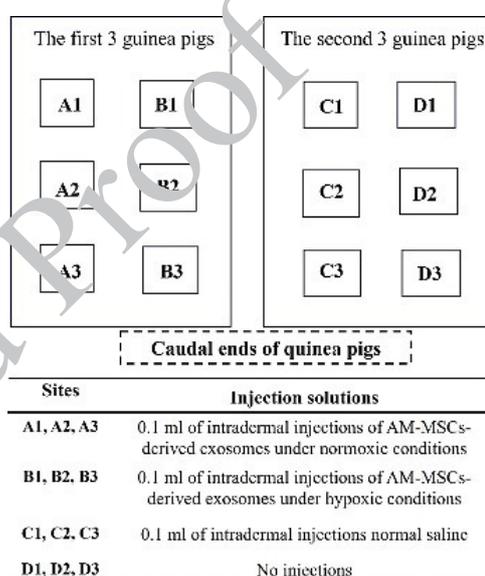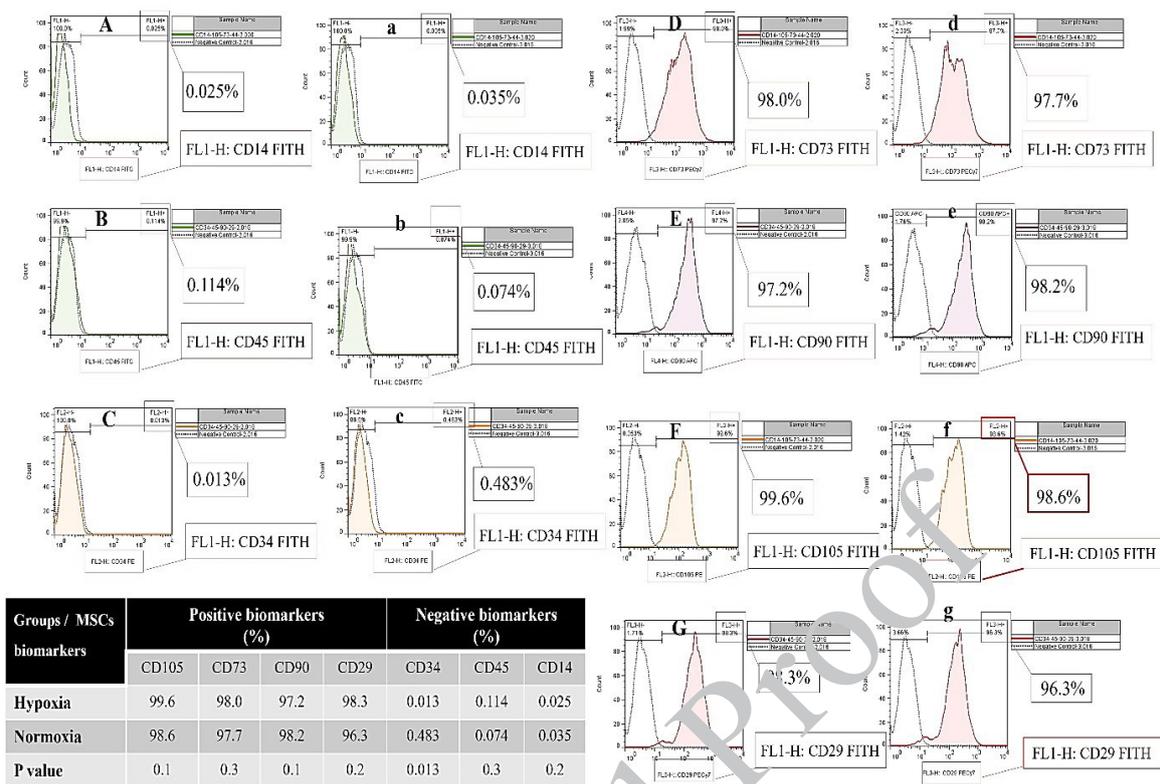

Figure 2. Intradermal injection sites and the corresponding solutions administered to guinea pigs at each site

Sites	Injection solutions
A1, A2, A3	0.1 ml of intradermal injections of AM-MSCs-derived exosomes under normoxic conditions
B1, B2, B3	0.1 ml of intradermal injections of AM-MSCs-derived exosomes under hypoxic conditions
C1, C2, C3	0.1 ml of intradermal injections normal saline
D1, D2, D3	No injections

Table 4. Magnusson and Kligman grading system

Patch test reaction	Grading scale
No visible change	0
Discrete or patchy erythema	1
Moderate and confluent erythema	2
Intense erythema and/or swelling	3

as negative molecular markers between the two groups (Figure 3, *P*>0.05). The expression of CD34 biomarkers under hypoxia was significantly decreased compared to the normoxic condition (0.013% vs. 0.483%, *P*≤0.05).

Morphological characterization of AM-MSCs-exosomes using SEM

Figure 4 demonstrates the size, surface topography, and surface shape of AM-MSCs-Exosomes under normoxic

| Groups / MSCs biomarkers	Positive biomarkers (%)				Negative biomarkers (%)		
	CD105	CD73	CD90	CD29	CD34	CD45	CD14
Hypoxia	99.6	98.0	97.2	98.3	0.013	0.114	0.025
Normoxia	98.6	97.7	98.2	96.3	0.483	0.074	0.035
P value	0.1	0.3	0.1	0.2	0.013	0.3	0.2

Figure 3. Expressions of CD14 (A, a), CD45 (B, b), CD34 (C, c), CD73 (D, d), CD90 (E, e), CD105 (F, f), and CD29 (G, g) molecular markers between both the normoxic (A-F) and hypoxic (a-f) conditions

(A-D) and hypoxic (a-d) conditions. Additionally, the histograms showing the size and distribution of exosomes under normoxic (D) and hypoxic (d) conditions are demonstrated in Figure 4. The exosomes extracted from both conditions maintained their typical round morphology. AM-MSCs-Exo in the hypoxic group exhibited a homogeneous appearance with an average size of 145 ± 15 nm. However, those from the normoxic group had an average size of 180

± 79 nm ($P \leq 0.05$, Figure 4). The normoxic group exhibited a significantly greater distribution size of AM-MSCs-Exo compared to the hypoxic group ($P \leq 0.05$, Figure 4).

Dispersion and aggregation of AM-MSCs-exosomes using TEM

Structural characteristics, dispersion, and aggregation of AM-MSCs-Exosomes in the normoxic (A, C) and
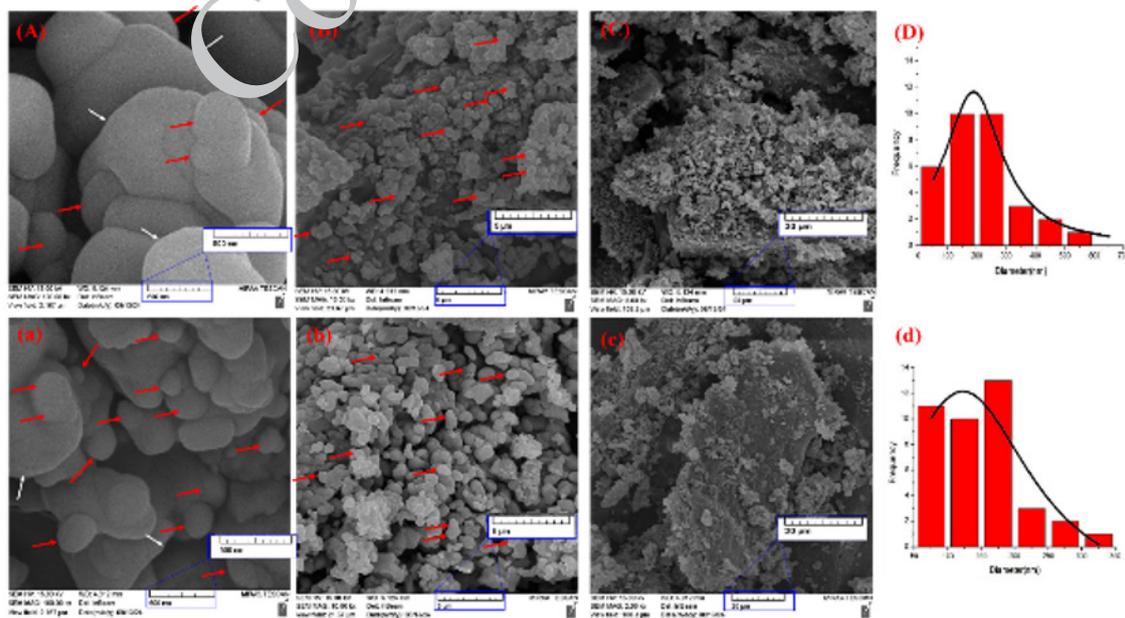
Figure 4. Morphological characterization of AM-MSCs-Exosomes in the normoxic (A-D) and hypoxic (a-d) conditions using SEM at magnifications of 500 nm, 5 μm, and 20 μm
Red arrows indicate exosomes, while white arrows probably represent ectosomes.
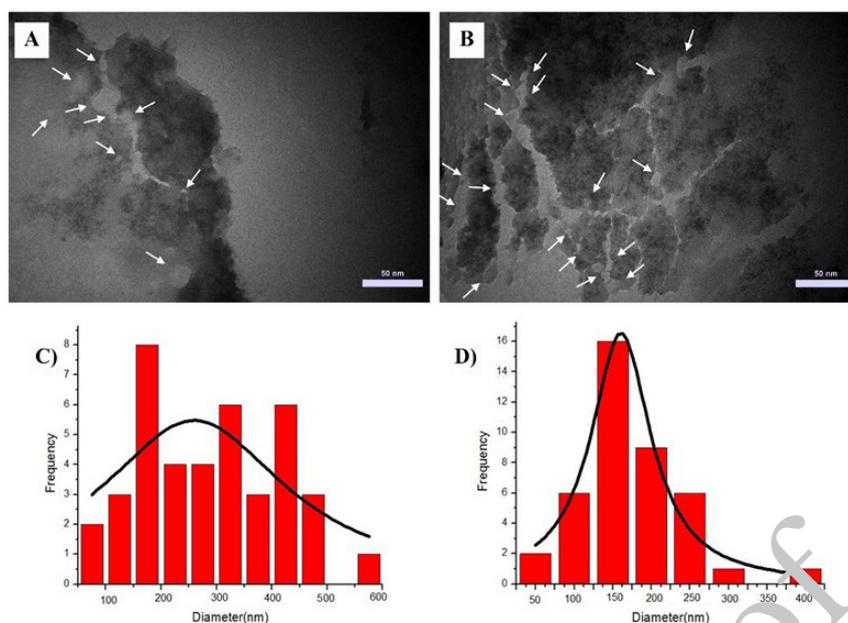
Figure 5. Structural characteristics and dispersion histograms of AM-MSCs-Exosomes under normoxic (A, C) and hypoxic (B, D) conditions, as observed by TEM at a magnification of 50 nm.

hypoxic (B, D) groups are shown in Figure 5. Exosomes appeared as hollow spheres (white arrows, Figures 5A and 5B) surrounded by a lipid layer. The distribution size and aggregation of AM-MSCs-derived exosomes in normoxia were significantly greater than those in the hypoxic group ($P \leq 0.05$, Figure 5).

Chemical features of AM-MSCs-exosomes using FTIR

Chemical composition and functional groups of AM-MSCs-Exosomes under hypoxic and normoxic conditions are shown in Figure 6. Additionally, Table 5 describes the peaks, wavelengths, and their interpretations, particularly the functional groups related to the extracted exosomes. FTIR analysis of the extracted exosomes revealed the presence of multiple compounds, including proteins (indicated by amide I and II peaks), lipids (aliphatic C-H peaks), glycoproteins or phospholipids (C-O or P-O peaks), and nucleic acids (P-O peak). Notably, the peak intensity in exosomes derived from hypoxic conditions showed a significant increase compared to those from normoxic conditions ($P \leq 0.05$, Figure 6). The variations in intensity of protein- and lipid-related peaks may indicate changes in their respective ratios. Additionally, changes in the peaks associated with protein secondary structure at 1646 and 1654 cm^{-1} positions may reflect structural alterations resulting from hypoxia.

Dimension and behavior of colloidal particles using DLS

Figure 7 demonstrates the size and behavior of colloidal particles under hypoxic and normoxic conditions. The
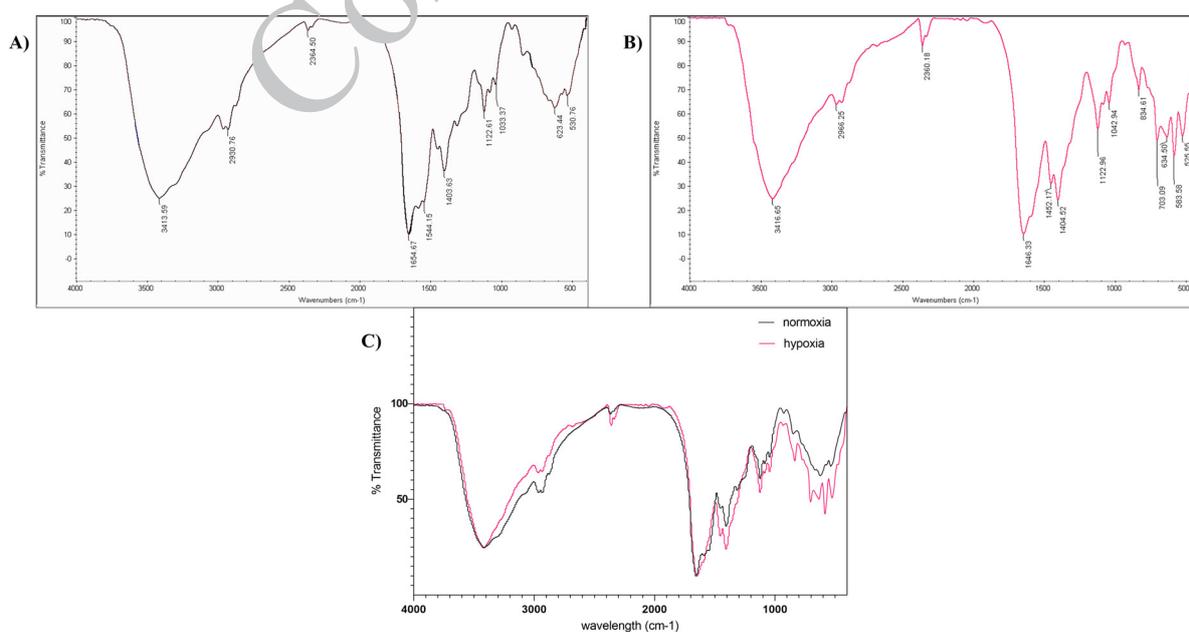
Figure 6. FTIR analysis of AM-MSCs-Exosomes under normoxia (A), hypoxia (B), and their comparison (C).

Table 5. Ionic interactions and relevant functional groups using FTIR analysis

Wavelength (cm^{-1})	Bond	Functional groups
3413	O-H stretching bond and N-H stretching bond	Alcohols, Amines, and Amides
2930	C-H asymmetric stretching bond	Methylene groups (CH$_2$) in aliphatic chains
2360	C=O=C asymmetric stretching bond	CO$_2$
1646	C=O stretching bond	Amide I in Proteins
1544	N-H Bending bond and C-N stretching bond	Amide II in Proteins
1446	C-H Bending bond	Methylene (CH$_2$) and Methyl (CH$_3$) groups
1404	COO- symmetric stretching bond	Carboxylates
1122	C-O stretching bond or P-O stretching bond	Alcohols, Ethers, Ester, or Phosphates
623	C-H out-of-plane bending bond	Aromatic cycles
525	C-X stretching bond or S-S stretching bond	Halides, disulfide bonding

average size of AM-MSCs-Exo in the normoxic group was 185.7 ± 23 nm (PI=0.756), while it was 145.4 ± 36 nm (PI=0.420) in the hypoxic group ($P\leq0.05$). The lower PI in the hypoxic condition indicates a more uniform distribution compared to the normoxic group, indicating that hypoxia-activated AM-MSCs-Exosomes are more dimensionally consistent than those in the normoxic group. These results also support the results of SEM and TEM analyses. Figures 4 and 5). The distribution and average particle size of AM-MSCs-Exosomes in the normoxic group were significantly higher than those observed under hypoxic conditions ($P\leq0.05$). Figure 7 (C, D) also demonstrates the fluctuation under scattered light (in terms of time) in the hypoxic and normoxic conditions. The normoxic group exhibited greater fluctuations compared to the hypoxic group, indicating an increase in particle size over time ($P\leq0.05$).

Zeta potential and stability of AM-MSCs-exosomes

Figure 7 demonstrates the surface charge and stability of exosomes in the normoxic and hypoxic groups. There was a significant difference in the zeta potential and stability of AM-MSCs-Exosomes between the two groups ($P\leq0.05$, Figure 7E). The zeta potential of AM-MSCs-Exosomes in the normoxic condition was -12.57 ± 0.5 mV, compared to -2.37 ± 0.73 mV in the hypoxic group. Figure 7E; $P\leq0.05$). Fluctuation-delay time analyses. Figure 7C, D) indicate that exosomes under hypoxia remained stable over time without noticeable agglomeration, whereas normoxic exosomes displayed increasing fluctuations over time, suggesting
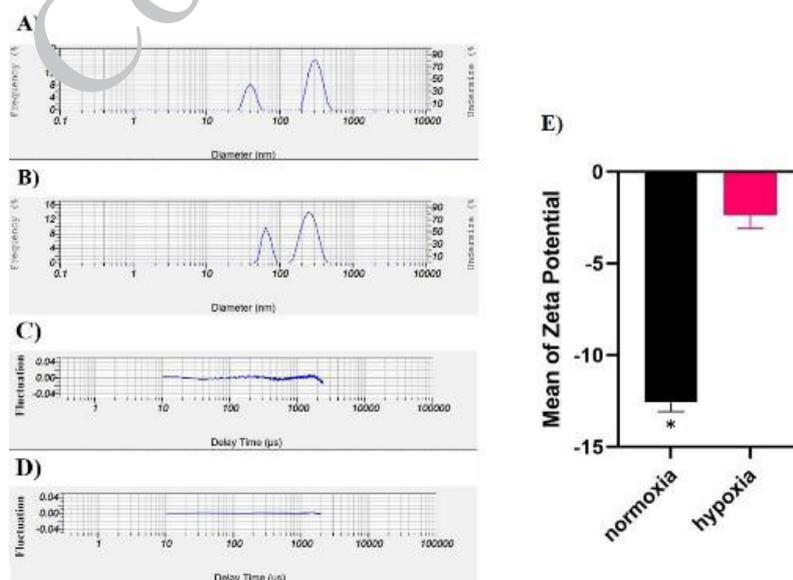
Figure 7. Size distribution and dynamic behavior of colloidal particles in the normoxic (A) and hypoxic (B) groups. Light scattering fluctuation of AM-MSCs-Exosomes under scattered light in the normoxic (C) and hypoxic (D) conditions
Zeta potential analysis of AM-MSCs-derived exosomes in different experimental groups (E). *P-value≤0.05.

Table 6. Microbiological quality analysis of rabbit AM-MSCs-Exosomes in various culture conditions

Description	Limits	Hypoxic group	Normoxic group
Average TAMC (CFU/g)	NA	<10	<10
Average TYMC (CFU/g)	NA	<10	<10
E. coli	Absence	Absence	Absence
S. aureus	Absence	Absence	Absence
P. aeruginosa	Absence	Absence	Absence
Salmonella sp.	Absence	Absence	Absence
C. albicans	Absence	Absence	Absence
Clostridia sp.	Absence	Absence	Absence
Bile-tolerant gram-negative bacteria	Absence	Absence	Absence

TAMC: Total aerobic microbial count; TYMC: Total combined yeasts and molds; CFU: Colony-forming unit

progressive agglomeration (Note: the continuous straight line in the hypoxia group (7D) and the oscillating uneven line in the normoxia group (7C), $P \leq 0.05$). These findings were also supported by TEM and DLS analyses, which confirmed the structural integrity and consistency of exosomes under both conditions.

Total protein concentration

The average total protein concentration of AM-MSCs-Exo was 4.109 mg/ml in the normoxic group, compared to 5.003 mg/ml hypoxia, a 1.22-fold increase in protein concentration due to hypoxia ($P \leq 0.01$). This suggests that inducing a hypoxia for AM-MSCs enhances total protein concentration.

Biocompatibility
Microbiological quality of AM-MSCs-Exosomes

Table 6 presents the results of microbiological analyses of AM-MSCs-Exosomes in the hypoxic and normoxic groups. There was no contamination (TAMC, TYMC, Gram-negative and positive bacteria, yeast, molds, etc.) in the extractions under hypoxia and normoxia.

Cytotoxicity of exosomes in the hypoxic and normoxic conditions

MTT confirmed the cytocompatibility of AM-MSCs-Exosomes in the hypoxic and normoxic groups on the L-929 fibroblast cell line, indicating their biocompatibility according to ISO 10993-5 (Table 7). L-929 fibroblast cells in the control group showed a baseline viability of 100 ± 12.3%. The addition of exosomes at a higher concentration (20μg/ml) to the culture medium significantly increased the survival rate in both hypoxic and normoxic groups, reaching 134.72 ± 7.8 % and 119.7 ± 8.4, respectively ($P \leq 0.05$). Between the two groups and various concentrations, the highest viability rate was observed in the hypoxic group at 20μg/ml ($P \leq 0.05$, Table 7). In contrast, no significant difference in cell viability was demonstrated between lower exosome concentrations and the control group ($P > 0.05$, Table 7).

In vivo irritation of exosomes from the normoxia- and hypoxia-activated AM-MSCs

Injection of exosomes from the normoxic- and hypoxic-activated AM-MSCs caused no edema, erythema, or eschar formation in male New Zealand rabbits; the total score was

Table 7. Optical densities (A) and cytocompatibility (B) of AM-MSCs-derived exosomes on the L-929 cell line under normoxic and hypoxic conditions at different concentrations (20, 15, 10, and 5 μg/ml) using the MTT assay

(A)

Repetition	Control	Hypoxic condition				Normoxic condition			
		20	15	10	5	20	15	10	5
1	0.7095	0.926	0.786	0.625	0.65	0.796	0.62	0.5	0.49
2	0.78	0.981	0.923	0.814	0.725	0.952	0.745	0.52	0.5
3	0.923	0.961	0.818	0.712	0.564	0.8	0.635	0.564	0.52

(B)

Control	Hypoxic condition (μg/ml)				Normoxic condition (μg/ml)			
	20	15	10	5	20	15	10	5
100±12.3[A]	134.72±7.8[B]	118.06±9.8[C]	101.06±5[A]	97.09±4.6[A]	119.7±8.4[C]	104.96±4.1[A]	101.41±6.2[A]	94.94±8[E]

Different superscript letters (A–E) indicate statistically significant differences between groups ($P \leq 0.05$).

Table 8. *In vivo* irritation results of exosomes under normoxic and hypoxic conditions following injection into male New Zealand rabbits

Skin reactions	Times	Normoxic conditions	Hypoxic conditions
Erythema	4 hr	0	0
	24 hr	0	0
	48 hr	0	0
	72 hr	0	0
Edema	4 hr	0	0
	24 hr	0	0
	48 hr	0	0
	72 hr	0	0
Eschar formation	4 hr	0	0
	24 hr	0	0
	48 hr	0	0
	72 hr	0	0

Table 9. Sensitization analyses of exosomes from normoxia-and hypoxia-activated AM-MSCs in the guinea pigs

Normoxic conditions		Hypoxic conditions	
Erythema	0	Erythema	0
Edema	0	Edema	0
Total	0	Total	0

zero for both groups. Table 8 indicates that AM-MSCs-Exosomes under normoxic and hypoxic conditions don't induce skin reactions after 4, 24, 48, and 72 hr.

***In vivo* sensitization of exosomes in the hypoxic and normoxic conditions**

According to the Magnusson and Kligman grading system, no edema, swelling, or erythema was observed after intradermal exosome injection under hypoxic and normoxic conditions (Table 9). Sensitization analysis demonstrates that exosomes from the normoxic-and hypoxic-activated AM-MSCs do not cause skin reactions in male Albino guinea pigs after three weeks.

Discussion

This study demonstrates that hypoxic preconditioning exerts significantly positive effects on the characteristics and quality of AM-MSC-derived exosomes. Specifically, hypoxia enhanced the morphological characteristics, structural properties, chemical features, and biological capacities of exosomes. These improvements suggest that hypoxic preconditioning can potentiate the therapeutic efficacy of exosomes in various medical fields, particularly regenerative medicine, immunomodulation, and targeted drug delivery. In the study, the average exosome size decreased to 145.4 ± 36 nm, accompanied by a uniform distribution (PI = 0.42) under hypoxic conditions. In contrast, the normoxic conditions produced larger exosomes, averaging 185.7±23 nm with a broader distribution (PI = 0.756). Additionally, the Zeta potential of AM-MSCs-Exo was -12.57 ± 0.5 mV under normoxia, while it was -2.37 ± 0.73 mV in hypoxic conditions. We demonstrated that the exosomes

from hypoxia-treated cells exhibited greater uniformity, dispersion, and stability than those from the normoxic group, resulting in reduced fluctuation under scattered light over time. These findings are consistent with several studies that have confirmed hypoxia improves the size and surface topography of exosomes (32). However, some researchers have noted that hypoxia improves the quality of exosomes without affecting their size (41, 42). These variations may be due to differences in cell sources, isolation and processing methods, analytical accuracy, duration of hypoxia, oxygen concentration, and timing of exosome collection post-treatment. Our results demonstrate that AM-MSCs-Exosomes cultured under hypoxic conditions exhibit greater temporal stability compared to normoxic exosomes. While the hypoxic exosomes displayed a lower zeta potential, this did not correlate with reduced stability, highlighting that zeta potential alone does not fully account for colloidal stability; as long as the repulsion is sufficient to maintain a potential energy barrier, the colloid remains stable (43, 44). The fluctuation-delay time analyses clearly show increased aggregation in the normoxic group, whereas hypoxic exosomes maintained consistent particle distribution over time. The precise mechanisms underlying the enhanced stability of hypoxic exosomes were not directly investigated in this study. Although factors such as Van der Waals forces, steric stabilization, or other interparticle interactions may contribute to colloidal stability (44), these remain hypotheses requiring further experimental validation. Future studies employing targeted biophysical measurements of interparticle forces could clarify the contributions of these mechanisms. Overall, these findings indicate that hypoxic culture conditions may improve the stability of AM-MSCs-Exosomes, reducing the propensity for agglomeration, and suggest a potential role for hypoxia in modulating the physicochemical properties of exosomes. This finding is consistent with prior reports demonstrating that hypoxia influences the physicochemical characteristics of colloidal systems, primarily through modifications in exosomal membrane composition and cargo (32, 45, 46).

In the study, the chemical composition of AM-MSCs-Exo was evaluated through FTIR analyses. The intensities of peaks representing proteins, lipids, phospholipids, glycoproteins,

and nucleic acids were increased in the hypoxic group, which means the concentration of these compounds can be increased under hypoxic conditions. The BCA assay confirmed the higher concentration of proteins for the hypoxic group. These results are consistent with previous studies. FTIR was suggested as a useful tool for the chemical evaluation of extracted exosomes, so that carbohydrates, phospholipids, DNA and RNA, proteins, and lipids were detected from the same spectral peaks as our results (47). The research on the extracted exosomes from cancerous and healthy sources demonstrated different intensities of peaks between experimental groups (48). Several studies confirmed that the different isolation methods resulted in the alteration of the intensity of peaks related to lipids, carbohydrates, proteins, and nucleic acids (49, 50).These studies clarified that low concentrations of exosomes from both normoxic and hypoxic groups reduced cell viability, likely due to insufficient bioactive cargo, heterogeneity, lack of threshold activation, impurities, and possible alteration of exosome characteristics under hypoxia. Several plausible, non-exclusive mechanisms may explain this phenomenon. First, the biological effects of exosomes are dose-dependent. Protective or proliferative effects of vesicles are typically observed only when their concentration exceeds a defined threshold, indicating a dose-dependent biological response. Whereas lower exosome concentration may fail to activate critical survival cascades such as PI3K/Akt or MAPK and, in some contexts, may even expose pro-apoptotic signals. Second, the inherent heterogeneity of exosomes and their diverse bioactive cargo, including microRNAs, RNAs, proteins, lipids, and cytokines, means that their biological impact is highly context-dependent. Some cell-derived nanovesicles have demonstrated pro-apoptotic effects, particularly at lower doses, leading to growth inhibition or programmed cell death. This quality highlights the complexity of exosome-mediated signaling and its potential therapeutic implications. Third, insufficient therapeutic cargo or the presence of impurities in low-dose preparation may induce cellular stress upon uptake, contributing to reduced viability. At low concentrations, this uptake may still occur, but without delivering enough beneficial cargo. This can lead to metabolic burden or oxidative stress, especially in sensitive cells, resulting in decreased viability. Finally, under hypoxic conditions, cells are already stressed due to oxygen deprivation, and low exosome concentrations may be inadequate to counteract this damage. Similarly, in normoxia, low-dose exosomes might not provide additional survival signals and may even disrupt baseline homeostasis (51-55). Additionally, we demonstrated a significant decrease in CD34 expression under hypoxia compared with normoxia (0.013% vs. 0.483%). This reduction may be due to several interconnected mechanisms. Generally, hypoxia triggers cellular stress responses, including the activation of hypoxia-inducible factor 1-alpha (HIF-1α), which can reprogram gene expression and either suppress or activate the transcription of surface molecular markers. However, the magnitude and severity of these effects are modulated by various factors, including the severity of hypoxia (5%, 7%, 1% or ≤1% O_2 concentration), the duration of exposure (short-term or long-term), the type of hypoxia (continuous or intermittent), culture conditions, and the specific cell type or its differentiation stage. Collectively, these variables influence the structural, morphological, and functional characteristics of the cells. We explained

it in the discussion (56-58). In the present study, the total protein concentration in exosomes derived from AM-MSCs under hypoxic conditions was 1.22-fold higher than that of the normoxic group. This finding is supported by several studies that have investigated protein levels in exosomes under hypoxic conditions, demonstrating that hypoxia increases protein concentration (59-61). de Jong et al. (62) demonstrated that hypoxic conditions modify the protein and RNA cargo of exosomes, thereby influencing their biological functions. It is well established that the hypoxia-inducednup-regulation of exosomal proteins affects cancer diagnosis (63) and treatment (64), and wound healing (65, 66). Mo et al. (63) reported that hypoxic exosomes possess an effective biomarker due to their protein content. Deep et al. in 2020 (64) suggested that the hypoxic exosomes affect the control of prostate cancer cell metastasis. Moreover, the elevated protein content of exosomes derived from hypoxia-treated cells is involved in multiple signaling pathways of extracellular matrix regeneration (65) and angiogenesis (66), highlighting their promising therapeutic potential in tissue repair and wound healing. Induction of stress in various cell lines (such as adipose derived MSCs (60), endothelial cells (62), macrophages (59), and glioma cells (40) through hypoxia alter the protein concentrations, resulting in changes in their biological functions. AM-MSCs-Exo produced under hypoxic conditions show improved physicochemical properties and biocompatibility. The higher protein concentration in the hypoxic group, along with its stability and the absence of sensitization and irritation indicates its potential for therapeutic applications.

Limitations and Future Directions

Despite the promising findings about the effect of hypoxia on the morphological characteristics, structural properties, chemical features, biological capacities, and biocompatibility of exosomes derived from AM-MSCs, several limitations should be acknowledged in this study. First, this study primarily focused on the physicochemical and biocompatibility of exosomes derived from AM-MSCs in vitro conditions, without exploring their functional validation or therapeutic efficacy in disease-specific models. Therefore, the therapeutic efficacy of hypoxia-derived AM-MSCs-Exo in vivo (both in preclinical models and clinical trials) remains to be validated. Second, while hypoxic conditions improved both the quality and quantity of exosomes, the molecular mechanisms and signaling pathways responsible for these improvements have not been investigated and warrant comprehensive investigation. Additionally, we evaluated only two oxygen concentrations (1% and 22%), leaving open the possibility that other oxygen tensions (different oxygen concentrations), or exposure durations, or multiple hypoxia applications (continuous or intermittent) could yield different or potentially superior outcomes. Other limitations include the sample size and donor variability, as well as the long-term stability of AM-MSCs-Exo, which may influence reproducibility and translational applicability. Moreover, the absence of functional assays, including those evaluating immunomodulatory, angiogenesis, anti-inflammatory, anti-tumor, anti-apoptotic, cargo delivery, or regenerative activities, restricts the interpretation of therapeutic potential beyond physicochemical properties. Future studies should include in vivo validation of therapeutic effects in relevant disease models, molecular pathways in exosome biogenesis,

comparative analysis across different hypoxic levels and durations, functional assays, and standardization protocols for production and scalability of clinical-grade exosomes. Addressing these aspects will strengthen the translational relevance of hypoxia-conditioned AM-MSCs-derived exosomes and support their development as advanced cell-free therapeutics. To overcome these limitations, future studies should be designed to validate the therapeutic effects of exosomes *in vivo* in relevant disease models, identify molecular pathways of exosome biogenesis, investigate different levels and duration of oxygen concentration, perform functional assays of produced exosomes, and standardize the exosome production protocol and scalability at the clinical level. Addressing these gaps will be critical for advancing AM-MSCs-Exo as a next-generation, cell-free therapeutic platform."

Conclusion

Hypoxic preconditioning enhances the yield and physicochemical stability of AM-MSC-derived exosomes, due to their unique composition and functional properties. Hypoxia improves the size, uniformity, morphology, size distribution, stability, and protein concentration of exosomes. Therefore, hypoxia can be used as an effective approach to enhance the quality of AM-MSCs and extracted exosomes for therapeutic applications.

It is recommended that future studies be designed to investigate the effect of long-term hypoxia and different oxygen concentrations on the quality of cell derivatives, as well as the molecular mechanisms and signaling pathways involved in exosome biogenesis. Additionally, conducting comprehensive functional assays, such as assessments of immunomodulatory, anti-inflammatory, anti-tumor, anti-apoptotic, angiogenic, cargo delivery, and tissue regenerative capacities, is essential to determine the therapeutic potential of exosomes. Furthermore, the standardization of exosome production, critically, and the scalability of clinical-grade exosome manufacturing play a critical role in enhancing their translational and therapeutic applicability. Addressing these aspects could pave the way for the development of hypoxia-conditioned AM-MSC-derived exosomes as a next-generation, cell-free therapeutic platform.

Ethics Approval

All procedures performed in studies involving human participants were in accordance with the ethical standards of the institutional and/or national research committee and with the 1964 Helsinki Declaration and its later amendments or comparable ethical standards. The study was approved by the Ethics Committees at the Research Ethics Committees of Islamic Azad University, Science and Research Branch (approval ID: IR.IAU.SRB.REC.1403.081).

Authors' Contributions

H K and B H designed the experiments; H K, B H, and H J performed experiments and collected data; F E, K ZS, and B H discussed the results and strategy; F E prepared the draft manuscript and visualization. F E, B H, and NA revised and edited the article; B H, H J, and A S supervised, directed, and managed the study; H K, F E, H J, K ZS, N A, A S, and B H approved the final version to be published.

Conflicts of Interest

The authors declare that they have no competing interests or financial relationships that could influence the work reported in this article.

Declaration

The authors declare no competing interests. We have not used any AI tools or technologies to prepare the manuscript.

References

1. Spees JL, Lee RH, Gregory CA. Mechanisms of mesenchymal stem/stromal cell function. Stem Ce Res Ther 2016; 7:125.

2. Lee DE, Ayoub N, Agrawal DK. Mesenchymal stem cells and cutaneous wound healing: novel methods to increase cell delivery and therapeutic efficacy. Stem Cell Res Ther 2016; 7:37.

3. Vizoso FJ, Eiro N, Cid S, Schneider J, Perez-Fernandez R. Mesenchymal stem cell secretome: Toward cell-free therapeutic strategies in regenerative medicine. Int J Mol Sci 2017;18:1852.

4. Vishnubalaji R, Al-Nbaheen M, Kadalmani B, Aldahmash A, Ramesh T. Skin-derived multipotent stromal cells–an archrival for mesenchymal stem cells. Cell Tissue Res 2012; 350:1-12.

5. Nambu M, Bagheri M, Solhjou Z, Jahromi BM, Akrami M, Rohani L, *et al.* Adipose tissue derived mesenchymal stem cell (AD-MSC) promotes skin wound healing in diabetic rats. Diabetes Res Clin Pract 2011; 93:228-234.

6. Kemp KC, Hows J, Donaldson C. Bone marrow-derived mesenchymal stem cells. Leuk Lymphoma 2005; 46:1531-1544.

7. Ledesma-Martínez E, Mendoza-Núñez VM, Santiago-Osorio E. Mesenchymal stem cells derived from dental pulp: a review. Stem Cells Int 2016; 2016:4709572.

8. Kim EY, Lee K-B, Kim MK. The potential of mesenchymal stem cells derived from amniotic membrane and amniotic fluid for neuronal regenerative therapy. BMB Rep 2014; 47:135.

9. Heidari B, Shirazi A, Akhondi MM, Hassanpour H, Behzadi B, Naderi MM, *et al.* Comparison of proliferative and multilineage differentiation potential of sheep mesenchymal stem cells derived from bone marrow, liver, and adipose tissue. Avicenna J Med Biotechnol 2013; 5:104.

10. Schosserer M, Reynoso R, Wally V, Jug B, Kantner V, Weilner S, *et al.* Urine is a novel source of autologous mesenchymal stem cells for patients with epidermolysis bullosa. BMC Res Notes 2015; 8:1-12.

11. Dittmer J, Leyh B. Paracrine effects of stem cells in wound healing and cancer progression. Int J Oncol 2014; 44:1789-1798.

12. Zhang J, Guan J, Niu X, Hu G, Guo S, Li Q, *et al.* Exosomes released from human induced pluripotent stem cells-derived MSCs facilitate cutaneous wound healing by promoting collagen synthesis and angiogenesis. J Transl Med 2015; 13:1-14.

13. Lopez-Verrilli MA, Caviedes A, Cabrera A, Sandoval S, Wyneken U, Khoury M. Mesenchymal stem cell-derived exosomes from different sources selectively promote neuritic outgrowth. Neuroscience 2016; 320:129-139.

14. Bai L, Shao H, Wang H, Zhang Z, Su C, Dong L, *et al.* Effects of mesenchymal stem cell-derived exosomes on experimental autoimmune uveitis. Sci Rep 2017; 7:4323.

15. Mitchell R, Mellows B, Sheard J, Antonioli M, Kretz O, Chambers

D, *et al.* Secretome of adipose-derived mesenchymal stem cells promotes skeletal muscle regeneration through synergistic action of extracellular vesicle cargo and soluble proteins. Stem Cell Res Ther 2019; 10:1-19.

16. Kumar P, Kandoi S, Misra R, Vijayalakshmi S, Rajagopal K, Verma RS. The mesenchymal stem cell secretome: A new paradigm towards cell-free therapeutic mode in regenerative medicine. Cytokine Growth Factor Rev 2019; 46:1-9.

17. Lombardi F, Palumbo P, Augello FR, Cifone MG, Cinque B, Giuliani M. Secretome of adipose tissue-derived stem cells (ASCs) as a novel trend in chronic non-healing wounds: an overview of experimental *in vitro* and *in vivo* studies and methodological variables. Int J Mol Sci 2019; 20:3721.

18. Iranian Food and Drug Administration. Guideline for extracellular vesicle studies [Internet]. Tehran: Ministry of Health and Medical Education; 2025 [cited 2025 Mar 8]. No.: GUI-DPNA-BIO-012; SOP-DPNA-BIO-001. Available from: https://fdo.sbmu.ac.ir

19. Kalluri R, LeBleu VS. The biology, function, and biomedical applications of exosomes. Science 2020; 7:367.

20. Zhang J, Guan J, Niu X, Hu G, Guo S, Li Q, *et al.* Exosomes released from human induced pluripotent stem cells-derived MSCs facilitate cutaneous wound healing by promoting collagen synthesis and angiogenesis. J Transl Med 2015; 13:49.

21. Lopez-Verrilli MA, Caviedes A, Cabrera A, Sandoval S, Wyneken U, Khoury M. Mesenchymal stem cell-derived exosomes from different sources selectively promote neuritic outgrowth. Neuroscience 2016; 320:129-139.

22. Yáñez-Mó M, Siljander PRM, Andreu Z, Bedina Zavec A, Borràs FE, Buzas EI, *et al.* Biological properties of extracellular vesicles and their physiological functions. J Extracell Vesicles 2015; 4:27066.

23. Jeppesen DK, Fenix AM, Franklin JL, Higginbotham JN, Zhang Q, Zimmerman LJ, *et al.* Reassessment of exosome composition. Cell 2019; 177:428-445. e418.

24. Bec N, Bonhoure A, Henry L, Berry L, Larroque C, Coux O, *et al.* Proteasome 19S RP and translation preinitiation complexes are secreted within exosomes upon serum starvation. Traffic 2019; 20:516-536.

25. Garcia NA, Ontoria-Oviedo I, González-King H, Diez-Juan A, Sepúlveda P. Glucose starvation in cardiomyocytes enhances exosome secretion and promotes angiogenesis in endothelial cells. PLoS One 2015; 10:e0138849.

26. Yang R, Li Z, Xu J, Luo J, Qu Z, Chen X, *et al.* Role of hypoxic exosomes and the mechanisms of exosome release in the CNS under hypoxic conditions. Front Neurol 2023; 14:1198546.

27. Jafari R, Rahbarghazi R, Ahmadi M, Hassanpour M, Rezaie J. Hypoxic exosomes orchestrate tumorigenesis: molecular mechanisms and therapeutic implications. J Transl Med 2020; 18:474.

28. Banerjee J, Sen CK. microRNA and wound healing. Adv Exp Med Biol 2015; 888:291-305.

29. Mu J, Li L, Wu J, Huang T, Zhang Y, Cao J, *et al.* Hypoxia-stimulated mesenchymal stem cell-derived exosomes loaded by adhesive hydrogel for effective angiogenic treatment of spinal cord injury. Biomater Sci 2022; 10:1803-1811.

30. Yuan N, Ge Z, Ji W, Li J. Exosomes secreted from hypoxia-preconditioned mesenchymal stem cells prevent steroid-induced osteonecrosis of the femoral head by promoting angiogenesis in rats. Biomed Res Int 2021; 2021:6655225.

31. Baglio SR, Rooijers K, Koppers-Lalic D, Verweij FJ, Pérez Lanzón M, Zini N, *et al.* Human bone marrow-and adipose-mesenchymal stem cells secrete exosomes enriched in distinctive miRNA and tRNA species. Stem Cell Res Ther 2015; 6:1-20.

32. He G, Peng X, Wei S, Yang S, Li X, Huang M, *et al.* Exosomes in the hypoxic TME: from release, uptake and biofunctions to clinical applications. Mol Cancer 2022; 21:19.

33. Liu W, Li L, Rong Y, Qian D, Chen J, Zhou Z, *et al.* Hypoxic mesenchymal stem cell-derived exosomes promote bone fracture healing by the transfer of miR-126. Acta Biomater 2020; 103:196-

212.

34. Wang J, Wu H, Peng Y, Zhao Y, Qin Y, Zhang Y, *et al.* Hypoxia adipose stem cell-derived exosomes promote high-quality healing of diabetic wound involves activation of PI3K/Akt pathways. J Nanobiotechnol 2021; 19:1-13.

35. Guo W, Qiao T, Dong B, Li T, Liu Q, Xu X. The effect of hypoxia-induced exosomes on anti-tumor immunity and its implication for immunotherapy. Front Immunol 2022; 13:915985.

36. Kumar A, Deep G. Exosomes in hypoxia-induced remodeling of the tumor microenvironment. Cancer lett 2020; 488:1-8.

37. Heidari B, Shams S, Akbari N, Zandsalimi K. Three-dimensionally decellularized human amniotic membrane scaffold: structure, processing, and biological properties. Cell Tissue Bank 2025;26:47.

38. Karimi M, Heidari B, Jafary H, Zandsalimi K. The quality and quantity of nanoparticles extracted from human adipose tissue-derived mesenchymal stem cells. Avicenna J Med Biotech 2025;17:186-195.

39. Rafighdoust Z, Baharara J, Forghanifard MM, Kerachian MA. Isolation and characterization of exosomes derived from breast cancer MDA-MB-231 cell line. Gene Cell Tissue 2021; 8:e110505.

40. United States Pharmacopeia Convention. United States Pharmacopeia 47–National Formulary 42 (USP 47–NF 42). Rockville (MD): United States Pharmacopeial Convention; 2024.

41. King HW, Michael MZ, Gleadle JM. Hypoxic enhancement of exosome release by breast cancer cells. BMC Cancer 2012; 12:421.

42. Zhang W, Zhou X, Yao Q, Liu Y, Zhang H, Dong Z. HIF-1-mediated production of exosomes during hypoxia is protective in renal tubular cells. Am J Physiol Renal Physiol 2017; 313:F906-F913.

43. Moore T, Rodriguez-Lorenzo L, Hirsch V, Balog S, Urban D, Jud C, *et al.* Nanoparticle colloidal stability in cell culture media and impact on cellular interactions. Chem Soc Rev 2015; 44:6287-6305.

44. Bhattacharjee S. DLS and zeta potential – what they are and what they are not? J Control Release 2016; 235:337-351.

45. Jiang H, Zhao H, Zhang M, He Y, Li X, Xu Y, *et al.* Hypoxia induced changes of exosome cargo and subsequent biological effects. Front Immunol 2022; 13:824188.

46. Ridolfi A, Cardellini J, Gashi F, van Herwijnen MJC, Trulsson M, Campos-Terán J, *et al.* Electrostatic interactions control the adsorption of extracellular vesicles onto supported lipid bilayers. J Colloid Interface Sci 2023; 650:883-891.

47. Ramos-Garcia V, Ten-Doménech I, Moreno-Giménez A, Gormaz M, Parra-Llorca A, Shephard AP, *et al.* ATR-FTIR spectroscopy for the routine quality control of exosome isolations. Chemom Intell Lab Syst 2021; 217:104401.

48. Zlotogorski-Hurvitz A, Dekel BZ, Malonek D, Yahalom R, Vered M. FTIR-based spectrum of salivary exosomes coupled with computational-aided discriminating analysis in the diagnosis of oral cancer. J Cancer Res Clin Oncol 2019; 145:685-694.

49. Dash M, Palaniyandi K, Ramalingam S, Sahabudeen S, Raja NS. Exosomes isolated from two different cell lines using three different isolation techniques show variation in physical and molecular characteristics. Biochim Biophys Acta Biomembr 2021; 1863:183490.

50. Kim JY, Rhim W-K, Yoo Y-I, Kim D-S, Ko K-W, Heo Y, *et al.* Defined MSC exosome with high yield and purity to improve regenerative activity. J Tissue Eng 2021; 12:20417314211008626.

51. Xiao Y, Zou D, Liu J, Dai F, Zhao A, Yang P. Dose-responsive effects of endothelial cell-sourced exosomes on vascular cell proliferation and phenotype transition. Biochim Biophys Acta Gene Subj 2025; 1869:130745.

52. Shi Y, Chen Y, Wang Y, Mo D, Ai H, Zhang J, *et al.* Therapeutic effect of small extracellular vesicles from cytokine-induced memory-like natural killer cells on solid tumors. J Nanobiotechnology 2024; 22:447.

53. Gurunathan S, Kang MH, Jeyaraj M, Qasim M, Kim JH. Review of the isolation, characterization, biological function, and multifarious therapeutic approaches of exosomes. Cells 2019; 8:307.

54. Tseng YJ, Huang HJ, Lin CH, Lin AM. A double-edged effect

of hypoxia on astrocyte-derived exosome releases. Exp Biol Med (Maywood) 2025; 250:10559.

55. El Sadik A, ALsaykhan HM, Alorini M, Hamouda N, Elzainy A. Prognostic impact of dose-dependent exosomes derived from mesenchymal stem cells. J Med Pharm Chem Res 2025;7:2689-2709.

56. Wu J, Yu L, Liu Y, Xiao B, Ye X, Zhao H, *et al.* Hypoxia regulates adipose mesenchymal stem cells proliferation, migration, and nucleus pulposus-like differentiation by regulating endoplasmic reticulum stress via the HIF-1α pathway. J Orthop Surg Res 2023; 18:339.

57. Eliasson P, Rehn M, Hammar P, Larsson P, Sirenko O, Flippin LA, *et al.* Hypoxia mediates low cell-cycle activity and increases the proportion of long-term–reconstituting hematopoietic stem cells during in vitro culture. Exp Hematol 2010; 38:301-310. e302.

58. Desplat V, Faucher J-L, Mahon FX, Sbarba PD, Praloran V, Ivanovic Z. Hypoxia modifies proliferation and differentiation of CD34+ CML cells. Stem Cells 2002; 20:347-354.

59. Jiang J, Wang W, Zhu L, Shi B, Chen Y, Xia Y, *et al.* Unveiling the role of hypoxic macrophage-derived exosomes in driving colorectal cancer progression. Front Immunol 2023; 14:1260638.

60. Li X, Fang S, Wang S, Xie Y, Xia Y, Wang P, *et al.* Hypoxia preconditioning of adipose stem cell-derived exosomes loaded in gelatin methacryloyl (GelMA) promote type H angiogenesis and osteoporotic fracture repair. J Nanobiotechnology 2024; 22:112.

61. Liu W, Rong Y, Wang J, Zhou Z, Ge X, Ji C, *et al.* Exosome-shuttled miR-216a-5p from hypoxic preconditioned mesenchymal stem cells repair traumatic spinal cord injury by shifting microglial M1/M2 polarization. J Neuroinflammation 2020; 17:47.

62. de Jong OG, Verhaar MC, Chen Y, Vader P, Gremmels H, Posthuma G, *et al.* Cellular stress conditions are reflected in the protein and RNA content of endothelial cell-derived exosomes. J Extracell Vesicles 2012; 1:18396.

63. Mo F, Xu Y, Zhang J, Zhu L, Wang C, Chu X, *et al.* Effects of hypoxia and radiation-induced exosomes on migration of lung cancer cells and angiogenesis of umbilical vein endothelial cells. Radiat Res 2020; 194:71-80.

64. Deep G, Jain A, Kumar A, Agarwal C, Kim S, Leevy WM, *et al.* Exosomes secreted by prostate cancer cells under hypoxia promote matrix metalloproteinase activity at pre-metastatic niches. Mol Carcinog 2020; 59:323-332.

65. Thankam FG, Chandra I, Diaz C, Dilisio MF, Fleegel J, Gross RM, *et al.* Matrix regeneration proteins in the hypoxia-triggered exosomes of shoulder tenocytes and adipose-derived mesenchymal stem cells. Mol Cell Biochem 2020; 465:75-87.

66. Wang Y, Cen A, Yang Y, Ye H, Li J, Liu S, *et al.* miR-181a, delivered by hypoxic PTC-secreted exosomes, inhibits DACT2 by downregulating MLL3, leading to YAP-VEGF-mediated angiogenesis. Mol Ther Nucleic Acids 2021; 24:610-621.

67. Tomazin K. Characterization of exosomes from glioma cells under hypoxia [Internet]. Lund (Sweden): Lund University; 2015 [cited 2025 Dec 23]. Master's thesis. Available from: http://lup.lub.lu.se/student-papers/record/5271385.